Automatic Page-Turning Mechanism with Near-Field Electroadhesive Force for Linearly Correctable Imaging

Junseok Lee[a], Wonseok Jeon[a], and Hyunseok Yang*[a]

***Abstract*—Recently, demand for digitization of books has increased in tandem with the spread of portable devices for electronic books. However, in a number of invented book-scanning devices, pages are turned manually by users, or pricey three-dimensional cameras are needed for image correction. Our automatic page-turning mechanism employs near-field electroadhesive force to turn a single page. As the near-field electroadhesive force on the closest sheet of paper is far stronger than that on the second, only a single sheet of paper can be lifted. Using Fourier series expansion, we prove that regardless of the geometrical configuration of electrodes, the force ratio on the closest to the second is dominantly controlled by the period of the configuration. Based on this, a novel electrode configuration is designed aiming to give higher force ratio than the conventional interdigital patterns. The advantage of our mechanism in image processing is that perspective correction is compatible with our mechanism, hence not requiring devices for acquiring 3-D information to reconstruct images. Our automatic page-turning mechanism with a fair success rate and the reduced number of components shows that it is a promising method for automatic low-cost book-scanning devices.**

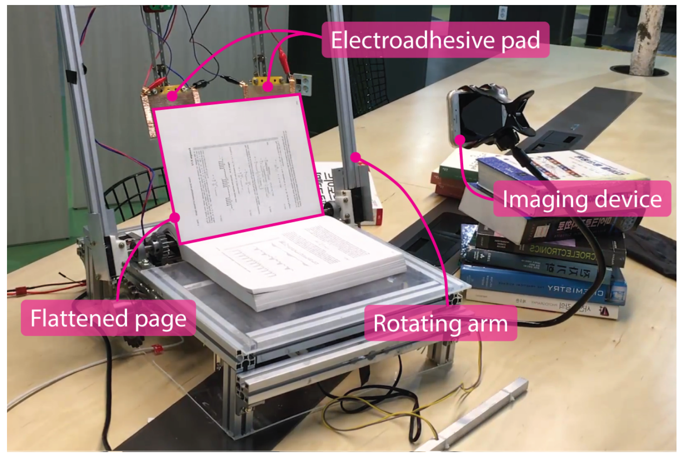

Fig. 1: The overview of the automatic page-turning machine equipped with the near-field electroadhesive pad.

I. Introduction

One common way to obtain information in the modern society is to read books. As books are not portable enough to carry and read, there has been demand for electronic books. However, electronic books did not meet the demand as the resolution of displays was too coarse to show fine fonts or figures. Along with the advances in high-resolution displays, reading electronic books on portable devices has become user-friendly. In this situation, plenty of devices for digitization of books, called book scanners, have been invented. However, most book scanners target industrial consumers such as companies, libraries, and schools, leaving behind personal consumers. To be used in big companies, the industrial book-scanning devices are needed to work at a high working speed, and thus equipped with complex components for page-turning mechanism and image processing. Although several personal book-scanners were invented, the function of automatic page-turning was excluded due to its complexity in the mechanism.

In this paper, we present automatic page-turning mechanism with near-field electroadhesive force for linearly correctable imaging [Fig. 1]. Our machine digitizes books in four steps. Firstly, only a single sheet of paper is lifted by simply placing a near-field electroadhesive pad on a page [Fig. 2(a)]. The rotating arm rotates to turn the page, and the page automatically flattens as the axes of rotation are asymmetrically arranged [Fig. 2(b)]. When flat enough for perspective correction, the page is imaged with a common camera [Fig. 2(c)]. After the page is released, the entire process is repeated [Fig. 2(d)]. The biggest difference from conventional book scanners is that it turns a page electronically, which is much simpler than turning it mechanically. In addition, our machine can take the advantages of linear image processing.

Electroadhesive force is an attractive force induced by the electrostatic interaction between electric fields and polarized dielectric materials. Using Fourier series, we prove that for any electrode configuration, the force ratio of the electroadhesive forces acting on the closest paper to the pad to the electroadhesive force on the second is dominated by the period of the configuration, especially on a small length-scale. A novel electrode configuration is designed to increase the force ratio. On the other hand, the acquired images from a camera are distorted around the bookbinding. Our mechanism employs perspective correction algorithm to rectifies the distortion, which is simple as it does not require topographic information. The simplicity in the page-turning mechanism and image processing makes our machine advantages for simplifying book-scanners.

[a] *School of Mechanical Engineering, Yonsei University, Seoul, Korea*

* Author to whom correspondence should be addressed. Corresponding email: hsyang@yonsei.ac.kr

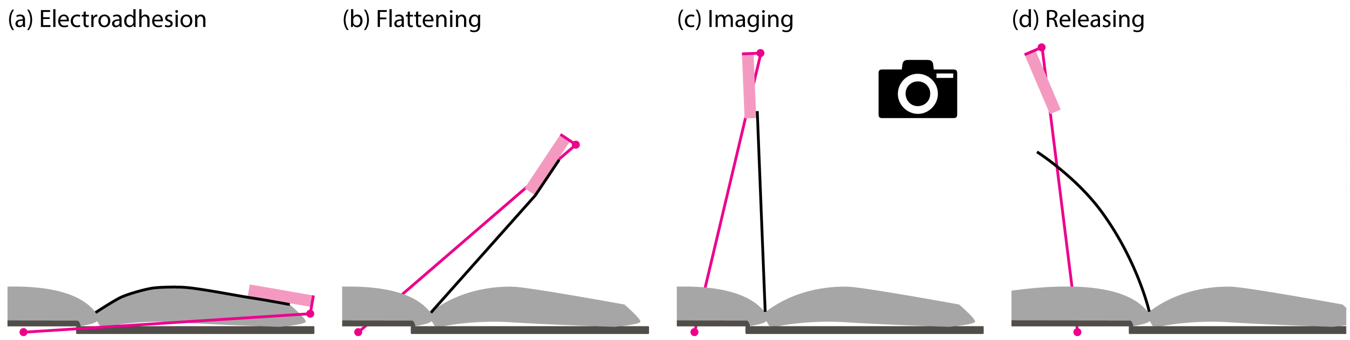

Fig. 2: Side views of book-scanning process. (a) A page is lifted up by near-field electroadhesive force. (b) Because the rotating arm and the paper rotate around different axes of rotation, the page becomes flat as it is turned. (c) When the page is positioned vertically, a picture of the page is taken and processed with perspective correction. (d) The book-scanning process is repeated after the page is detached.

II. Related technologies on and requirements for our mechanism

A. Book-turning mechanisms

The book-scanning method is classified into destructive and non-destructive types. The destructive book-scanners cut books into sheets of paper, and scan them with automatic document feeders. This type is simple and fast, but it is irreversible and unacceptable for some cases. The non-destructive types digitize books in a preserving way by turning and imaging each page. The non-destructive book-scanners are demonstrated by mechanically turning pages using roller structures [1], bionic fingers [2], vacuum pumps [3–7], and page turner heads [8]. In the scanner having roller structures, a roller is placed above a page and rotated to turn the page. In devices using vacuum pumps, the negative pressure generated by the pumps lifts up pages. However, vacuum pumps have noise, vibration, and energy inefficiency. Page turner heads precisely move a toe to release a single page as a human flips pages. In this mechanism, step motors with high spatial resolution are required with the elastic force of the paper and the support of air blast.

B. Electroadhesive force

Electroadhesive force is an attractive force that arises from the electrostatic interaction between an electric field and induced dipoles in dielectric materials. The electroadhesive force has widely been studied for application as a gripping force because of its many advantages. It is energy-efficient, does not involve noise and vibration, and is applicable regardless of the material properties of the object to be attached. The versatility of the electroadhesive force led to the development of wall-climbing robots [9–11], and perching mechanism of a robotic insect [12] in the field of robotics. For manipulation tasks, it is also applied to manipulation of arbitrary objects [13], fabrics [14], carbon fibers [15], unbound sheets of papers [16], and silicon wafers [17]. Thus far, the maximum force that electroadhesion can generate has mainly been studied [18]. The maximum force is, however, no longer important in the application of page-turning since a sheet of paper is usually light enough to lift. Instead, it becomes of importance how stronger the exerted force on the first page is than that on the second page, *i.e.*, the electroadhesive force should rapidly diminish to zero within the first page.

C. Imaging mechanisms

In most book scanners, image correction is performed to dewarp the distorted image of a page around the bookbinding. Topographic information is required to rectify the distorted images using mathematical models. It can be obtained with 3-D cameras [19, 20], or high-speed cameras [21]. In particular, if the page is perfectly flat, the topographic information is not needed, because it implies that the curvature is zero at all points. In this case, the distorted images can be rectified using the algorithm for perspective correction. The book scanners that utilize this usually use V-shaped structures for pressing books to flatten pages. The V-shaped structure is often made transparent with glasses, and pictures can be taken through it [2]. Yet, the glasses large enough to cover open books are hard for maintenance. To address this, book scanners using linear camera arrays have been developed [7, 22].

D. Requirements for our mechanism

We adopt perspective correction for simple image rectification. The digitization process of books is, then, required to satisfy the followings.

Accuracy: While the machine converts paper books into electronic documents, any pages should not be excluded. In our mechanism, one sheet of paper can be lifted up by near-field electroadhesive force realized with the extremely small length-scale.

Energy-efficiency: Since book-scanning processes usually run for a long time, energy consumption should be minimized. For example, turning pages with a vacuum pump consumes so considerable amount of energy that it is not appropriate for long use. By contrast, the electroadhesion employed in our device consumes minimal energy in the order of 3 W.

Flatness of paper: It is important to keep pages flat because the perspective correction is performed successfully with flat pages. Moreover, it should be able to keep a page flat for a certain period of time for an ordinary camera to take pictures.

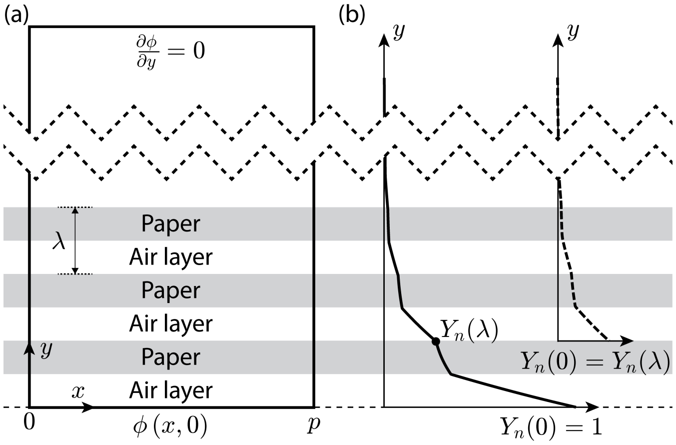

Fig. 3: A book is modeled as a stack of infinitely alternating sheets of paper and air layers. The white regions represent air layers, and the gray sheets of paper. (a) The domain and the boundary conditions for Laplace's equation. The domain is reduced to one period of the electrode configuration that is repeated in X-direction. (b) The function $Y_n(y)$ is scaled by $Y_n(\lambda)$ every λ.

In our mechanism, the near-field electroadhesive pad generates sufficient frictional force to flatten pages.

III. Near-field electroadhesive force

Electric fields which strongly depend on a distance from sources can be constructed by properly placing a set of charges. Specifically speaking, although a single charge forms an electric field whose magnitude depends only on $1/r^2$, the magnitude of the electric field by dipole depends on $1/r^3$, and further, that by quadrupole depends on $1/r^4$. One of the simplest configurations of positioning electric charges is an interdigitated pattern, which has positive and negative electrodes alternately. The electric field generated by the interdigitated pattern in a homogeneous medium can be analytically derived in the form of a power series under a couple of assumptions using Fourier series [23] or Green's function [24].

More generally, we analyze the decaying characteristics of the electric fields generated by any repeating electrode configuration in inhomogeneous space consisting of air layers and sheets of paper. The electroadhesive force on each sheet of paper is obtained by solving Laplace's equation and integrating Maxwell's stress tensor on their surfaces. Then, we calculate the ratio of electroadhesive force on the first page to that on the second page and finally show that the decaying nature depends on the very period of patterns.

We model pages of a book as infinitely many sheets of paper, between which air layers are embedded to roughly simulate the air layers formed by the rough surface of paper [Fig. 3(a)]. It is supposed that paper is linear, homogeneous, and neutrally charged, and the electrodes are long enough compared to the width. We limit our interest to the arbitrary configurations of electrodes that are continuously repeated with the period p and have the same positive and negative charges, so that the electric fields vanish at the infinite point.

On a quasi-static state, the electric field is obtained by solving Laplace's equation,

$$\nabla^2\phi = 0, \tag{1}$$

where ϕ represents the electric potential. As the configuration of electrodes is repeated, the potential is a periodic function with respect to x. Hence, at arbitrary height above the electrodes, say $y=0$, the potential can be expressed in the form of Fourier series as

$$\phi\left(x,0\right) = A_0 + \sum_{n=1}^{\infty}\left(A_n\cos\left(k_n x\right) + B_n \sin\left(k_n x\right)\right), \tag{2}$$

where $k_n = 2n\pi/p$, and A_n and B_n are Fourier coefficients. That the electric field diminishes to zero at infinity imposes on the top boundary

$$\mathbf{E}_y = -\frac{\partial\phi}{\partial y} = 0. \tag{3}$$

At the interfaces between paper domains and air domains, the following boundary conditions are imposed.

$$V_{\text{air}} = V_{\text{paper}}, \tag{4}$$
$$\varepsilon_{\text{air}}\frac{\partial V_{\text{air}}}{\partial y} = \varepsilon_{\text{paper}}\frac{\partial V_{\text{paper}}}{\partial y}. \tag{5}$$

From the separation of variables, $\phi_n(x,y) = X_n(x)Y_n(y)$, and the solution for Laplace's equation is expressed as

$$\phi\left(x,y\right) = A_0 Y_0(y) + \sum_{n=1}^{\infty} X_n\left(x\right) Y_n\left(y\right). \tag{6}$$

From Eqs. (1) to (3),

$$X_n(x) = A_n\cos\left(k_n x\right) + B_n\sin\left(k_n x\right), \tag{7}$$

and $Y_n(y)$ satisfies

$$\partial_y^2 Y_n(y) - k_n^2 Y_n(y) = 0, \tag{8}$$
$$Y_n(0) = 1, \tag{9}$$
$$\partial_y Y_n(\infty) = 0. \tag{10}$$

Also, from Eqs. (4) and (5),

$$Y_{n,\text{air}}\left(y\right) = Y_{n,\text{paper}}\left(y\right), \tag{11}$$
$$\varepsilon_{\text{air}}\frac{\partial Y_{n,\text{air}}}{\partial y} = \varepsilon_{\text{paper}}\frac{\partial Y_{n,\text{paper}}}{\partial y}. \tag{12}$$

As $Y_0(y)$ has a constant slope in each region of air layers and paper, if $Y_0'(y) \neq 0$, Eq. (10) cannot be satisfied. Hence, $Y_0(y) = 1$.

From Eqs. (8) to (12), Y_n can be obtained and decreases changing slopes at the interfaces [Fig. 3(b)]. If the boundary condition Eq. (11) is replaced with $Y_n(0) = Y_n(\lambda)$, the solution will be scaled as $Y_n(\lambda)Y_n(y)$ because the constitutive equations are linear. On the other hand, because the paper and air layers are infinitely stacked, even if the first paper and air layer are excluded, the solution does not change. Hence, $Y_n(y)$ is repeated every λ, being scaled by $Y_n(\lambda)$. When we define

$$Y_{nm}\left(y\right) \equiv Y_n\left(y + (m-1)\lambda\right) \qquad \text{for } y \in (0,\lambda), \tag{13}$$

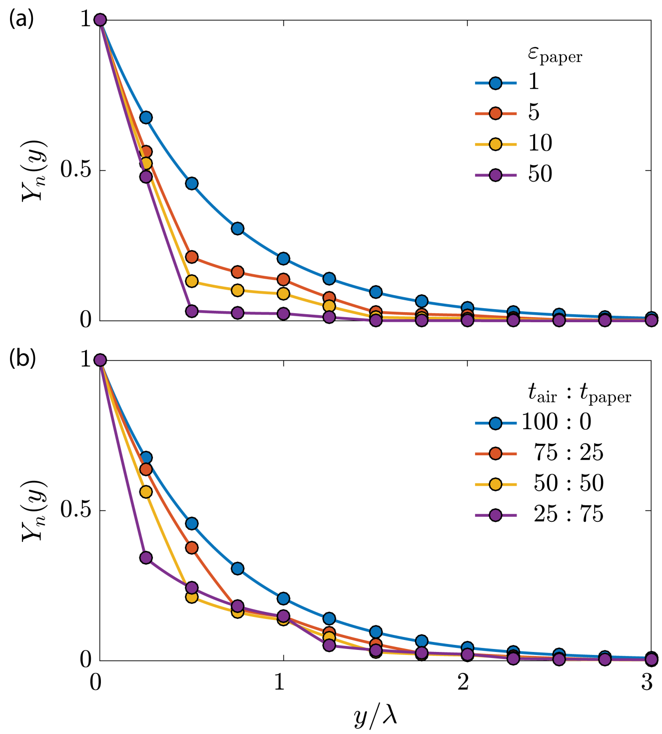

Fig. 4: **The effect of dielectric constant and the proportion of paper on the decay ratio.** (a) The high dielectric constant of paper decreases the decay ratio. (b) The decay ratio is minimized when a stack of papers and air layers occupy the equal spaces.

$Y_n(y)$ can be expressed as

$$\begin{aligned} Y_n(y) &= (Y_n(\lambda))^{[y/\lambda]} Y_{n1}\left(y - \lambda\left[\frac{y}{\lambda}\right]\right) \\ &= \alpha_n^{[y/\lambda]} Y_{n1}\left(y - \lambda\left[\frac{y}{\lambda}\right]\right), \end{aligned} \tag{14}$$

where the decay ratio $\alpha_n \equiv Y_n(\lambda)$. Plugging Eq. (14) into Eq. (12) at $y = \lambda$ gives

$$\begin{aligned} \varepsilon_{\text{paper}} Y'_{n1}(\lambda - 0) &= \varepsilon_{\text{air}} Y'_{n2}(+0) \\ &= \varepsilon_{\text{air}} \alpha_n Y'_{n1}(+0). \end{aligned} \tag{15}$$

By solving equations for Y_{n1}, one can obtain Y_n.

To characterize the decay ratio, Y_n is calculated for various dielectric constants of paper [Fig. 4(a)]. If $\varepsilon_{\text{paper}} = 1$, the domain is the same as if it was homogeneously filled with air, and we have $Y_n = e^{-k_n y}$ from Eqs. (8) to (10). When the paper has a higher dielectric constant, Y_n deflects downwards to satisfy Eq. (12) resulting in smaller decay ratio. The decay ratio is also estimated for different proportion of paper [Fig. 4(b)]. If space is filled only with air or paper, space becomes homogeneous for both cases, and thus, the solutions are equal. It is followed that the decay ratio is the smallest when air layers and paper equally occupy the space. For all cases, Y_n decays more rapidly than when space is filled with air. Hence,

$$\alpha_n \le e^{-k_n \lambda}. \tag{16}$$

From $\mathbf{E} = -\nabla\phi$, we have

$$E_x = -\sum_{n=1}^{\infty} \alpha_n^{[y/\lambda]} Y_{n1}\left(y - \lambda\left[\frac{y}{\lambda}\right]\right) X'_n(x), \tag{17}$$

$$E_y = -\sum_{n=1}^{\infty} \alpha_n^{[y/\lambda]} Y'_{n1}\left(y - \lambda\left[\frac{y}{\lambda}\right]\right) X_n(x), \tag{18}$$

and Maxwell stress tensor is computed as

$$\begin{aligned} T_{yy} &= \frac{1}{2}\varepsilon_0\left(E_y^2 - E_x^2\right) \\ &= \sum_{i,j=1}^{\infty} (\alpha_i\alpha_j)^{[y/\lambda]} T_{ij}\left(x, y - \lambda\left[\frac{y}{\lambda}\right]\right), \end{aligned} \tag{19}$$

where T_{ij} is defined as $\varepsilon_0(Y'_{i1}Y'_{j1}X_iX_j - Y_{i1}Y_{j1}X'_iX'_j)/2$. As T_{xy} does not contribute to the electroadhesive force, integrating only Eq. (19) over the surfaces of the first paper $S1$ gives the electroadhesive force acting on the first paper per the period, which are expressed as

$$F_{\text{1st}} = \oint_{S1} T_{yy}\,dx = \sum_{i,j=1}^{\infty} F_{ij}, \tag{20}$$

where

$$F_{ij} \equiv \oint_{S1} (\alpha_i\alpha_j)^{[y/\lambda]} T_{ij}\left(x, y - \lambda\left[\frac{y}{\lambda}\right]\right) dx. \tag{21}$$

As the surface of the second paper $S2$ is the translate of $S1$ in Y-direction by λ,

$$F_{\text{2nd}} = \oint_{S2} T_{yy}\,dx = \sum_{i,j=1}^{\infty} \alpha_i\alpha_j F_{ij}. \tag{22}$$

Thus, the ratio of the electroadhesive forces on the first paper to the second is

$$\frac{F_{\text{1st}}}{F_{\text{2nd}}} = \frac{F_{11} + F_{12} + \cdots}{\alpha_1\alpha_1 F_{11} + \alpha_1\alpha_2 F_{12} + \cdots}. \tag{23}$$

Since $\alpha_1\alpha_1$ is the maximum, from the mediant inequality,

$$\frac{F_{\text{1st}}}{F_{\text{2nd}}} \gtrsim \frac{1}{\alpha_1\alpha_1} \ge \exp\left(\frac{4\pi\lambda}{p}\right). \tag{24}$$

Therefore, independent of geometrical configuration of electrodes, the force ratio of the electroadhesive forces is lower-bounded by the ratio of the first-order terms, which depends on the period of electrode configuration. It implies that the period of electrode configuration should be reduced to increase the force ratio. The force ratio calculated from the first-order terms is valid when the high-order terms are negligible. Rewriting Eq. (24) gives

$$\delta \gtrsim 1, \qquad \delta \equiv \frac{p}{4\pi\lambda}\ln\left(\frac{F_{\text{1st}}}{F_{\text{2nd}}}\right), \tag{25}$$

where δ is the deviation that can be used as a quantity to measure how exact the force ratio obtained from the first-order approximation is. The deviation close to 1 indicates that the force ratio computed using the first-order terms is close to the force ratio obtained from the solution for homogeneous space.

Additionally, when the applied voltage is changed from V_0 to aV_0, the solution for Laplace's equation will then be changed from ϕ to $a\phi$. It is followed that the electroadhesive

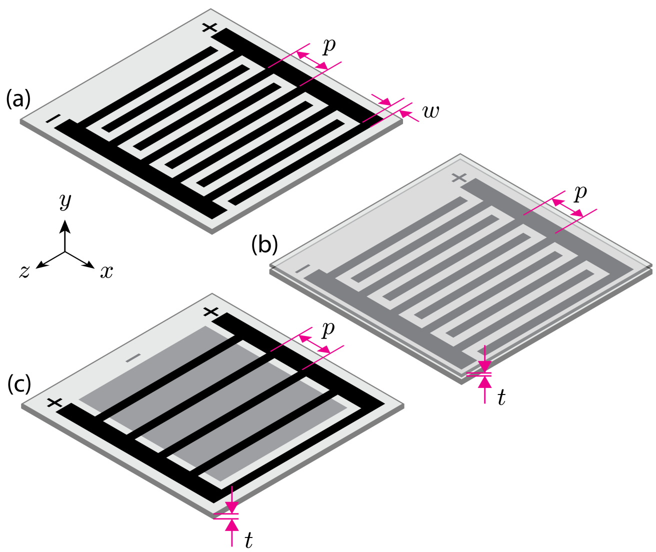

Fig. 5: **Three variations of interdigitated pattern and their control parameters.** (a) Pattern A. Both positive and negative electrodes are patterned on a substrate. The period and the width of the electrodes are varied. (b) Pattern B. Both electrodes are enclosed between a substrate and an insulating layer. The period and the thickness of the coating layer are controlled. (c) Pattern C. The positive electrodes are deposited on a substrate, and the ground beneath. The period and the thickness of the substrate are changed.

Material Properties				
All Pattern	Air layer			
	Relative permittivity	ε_{air}	1	–
	Thickness	t_{air}	50	µm
	Separation	t_{sep}	20, 50	µm
	Paper			
	Relative permittivity	$\varepsilon_{\text{paper}}$	2	–
	Thickness	t_{paper}	50	µm
Pattern A	Electrodes			
	Width/period	$w_{\text{electrode}}/p$	25–75	%
Pattern B	Coating layer			
	Relative permittivity	$\varepsilon_{\text{coating}}$	4	–
	Thickness	t_{coating}	100–500	µm
Pattern C	Substrate			
	Relative permittivity	$\varepsilon_{\text{subs}}$	4.8	–
	Thickness	t_{subs}	400–1200	µm

TABLE I: Properties used for the numerical estimation of electroadhesive forces.

force increases by constant times a^2. Hence, the force ratio is independent of the applied voltage.

Common electroadhesive pads include the interdigital pattern which alternately has positive and negative electrodes [Fig. 5(a)], and the interdigital pattern coated with insulating materials [Fig. 5(b)]. Based on the result that the force ratio is dominantly controlled by the period of a geometry on small length-scales, we design a novel electrode configuration that is aimed to decrease the period [Fig. 5(c)]. It is a double-sided structure that only has a positive digital pattern on a substrate, and the ground beneath. Despite having the same spacing between electrodes as interdigital patterns, it has a twice smaller period and higher force ratio. Another advantage is that the double-sided pattern is safer from dielectric breakdown than interdigital patterns, because the dielectric strength of a substrate is stronger than that of the air, and the thickness of the substrate can be controlled without changing the period.

Using COMSOL Multiphysics®, we perform numerical analysis to estimate the exact ratio of electroadhesive forces for the three kinds of electrode configurations with the material properties listed in Table I. For all patterns, the force ratios are calculated for different periods and separations that indicate the distance from a substrate to the closest page. Additional parameters are included depending on each configuration: the width of the electrodes for interdigital patterns, the thickness of the coating layer for the coated patterns, and the thickness of the substrate for the double-sided patterns. Considering the electric fields exponentially decay every period, the height of the computational domain is assigned to 10 times the period.

The results show that the force ratio can be increased by adjusting the period for all geometrical configurations [Figs. 6(a) to 6(c)]. The force ratio is multiplied particularly in the smaller period and increases as the separation decreases, and the effect of separation becomes negligible on small length-scales. For small separation, there is no enough distance for high-order terms of the electroadhesive force to vanish in the separation. The high-order terms have smaller decay ratio, only contributing to the electroadhesive force on the first paper. Hence, in order to increase the force ratio, the paper should be as close as possible to the electrodes, and the period must be reduced. For large periods, as the period increases, the force ratio continues to deviate from the approximate force ratio, because the high-order terms take a longer distance to diminish [Fig. 6(d)].

Practically, the electroadhesive pad is coated with insulating materials such as polymers that have high dielectric strengths to prevent dielectric breakdown in the air [25, 26]. With the insulating materials, one can avoid dielectric breakdown to apply the higher voltage to the electrodes to generate the stronger electroadhesive force. However, as the force ratio is of more importance than its magnitude in the page-turning application, contacting the first paper closer to the electrodes is advantageous in increasing the force ratio. Suppose the dielectric constant is small enough to be close to that of air. Then, the electroadhesive force in that surrounding equals the electroadhesive force with the separation of $t_{\text{sep}} + t_{\text{coating}}$. The increased separation decreases the force ratio. Moreover, the magnitude of the electroadhesive force on the first paper is too significantly dropped in the coating layer to exert sufficient force to lift a page, because near-field electroadhesion rapidly decays. Although the coating layer permits applying the higher voltage, electroadhesive force can be only increased in proportion to the square of the voltage. By contrast, the near-field electroadhesive force decreases exponentially. Therefore, it is critical to minimize the thickness of the coating layer.

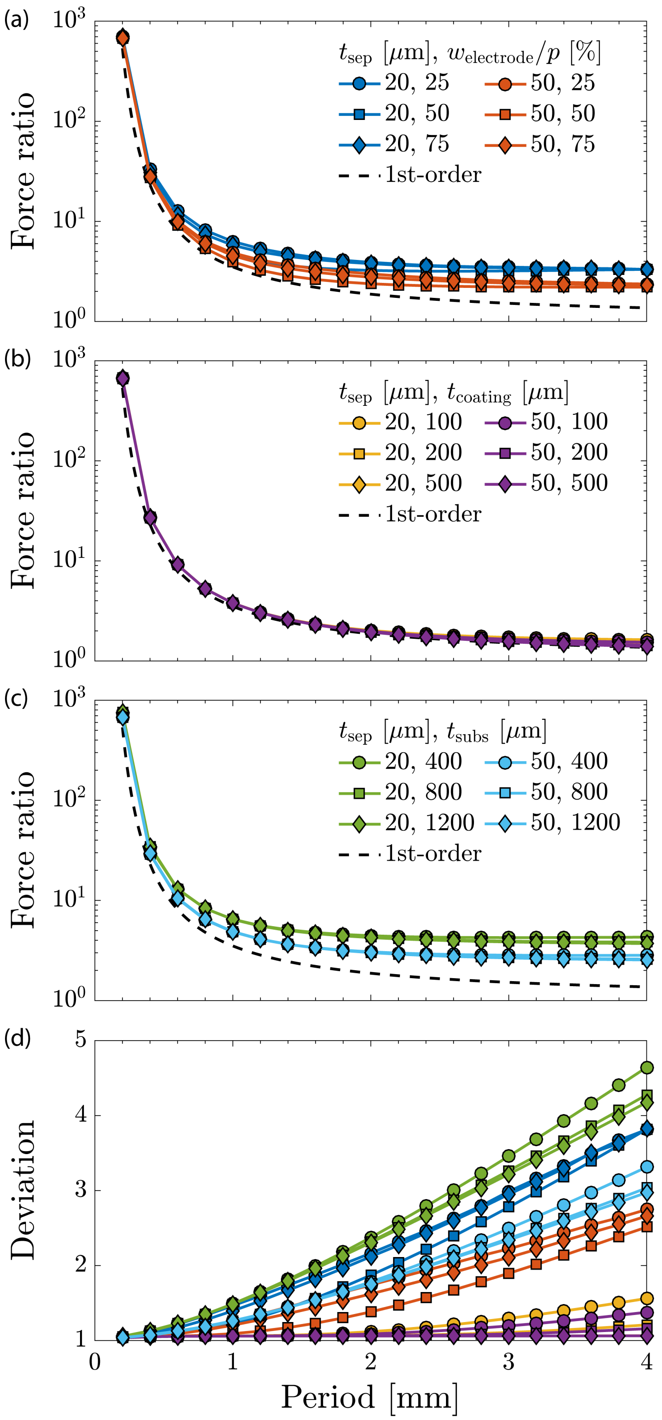

Fig. 6: **From top to bottom, the force ratios for the electrode configurations of pattern A, B, and C, and their deviations as a function of the period.** (a), (b), (c) When the period is small, the force ratios are dominantly affected by the period regardless of electrode configurations. When the periods are large or the separations are small, the force ratios are slightly greater than the force ratios from the first-order approximation due to the contribution of high-order terms. (d) The deviation shows that the force ratio calculated under the first-order approximation is fairly accurate for small periods.

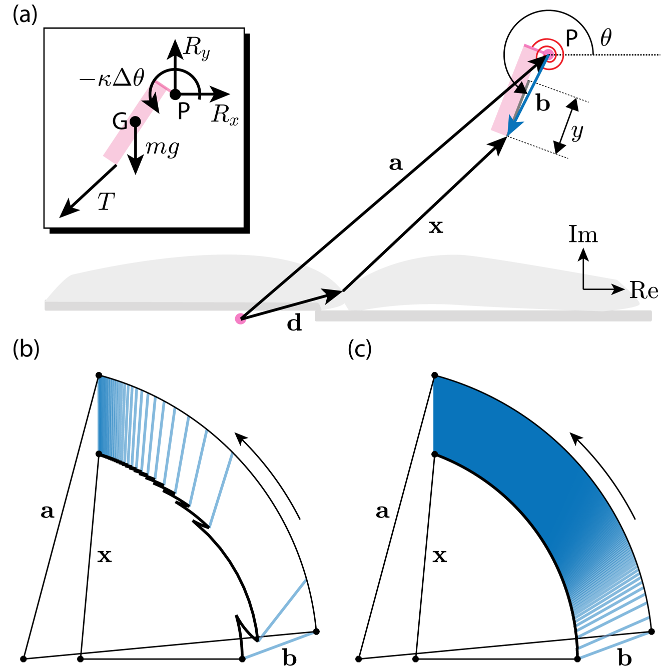

Fig. 7: **Dynamics of the near-field electroadhesive pad.** (a) A vector loop and a free body diagram of the electroadhesive pad (*inset*). (b) The trajectory of the electroadhesive pad (blue lines) shows that when the stiffness of the torsion spring is small, the motion becomes unstable as transition between stick and slip is repeated. (c) Stick-slip phenomenon is minimized with the high stiffness, because gravitational and elastic potential energy stored during stiction is reduced.

IV. Configuration of the Machine

A. Electroadhesive pad

The electroadhesive pad is attached with torsion spring to lift a page from the edge. It permits air entering into the gap, which reduces the force required to overcome the atmospheric pressure. The rotation axes of the rotating arm the paper are positioned differently, so that the paper naturally flattens by the friction while sliding out of the electroadhesive pad. However, a stick-slip phenomenon caused by the fiction makes unstable the motion of the electroadhesive pad. If the electroadhesive pad vibrates in a large angle due to the stick-slip instability, a large portion of the paper will slip out of the pad and no longer flatten. Therefore, stick-slip instability must be reduced to successfully flatten pages.

The motion of the electroadhesive pad can be described using four position vectors as

$$\mathbf{x} = \mathbf{a} + \mathbf{b} - \mathbf{d}, \qquad \mathbf{b} = be^{i\theta}, \tag{26}$$

where $\mathbf{x}$ represents the shortest path from the book spine to the electroadhesive pad [Fig. 7(a)]. The equation for the moment about P is expressed as

$$I_{\mathrm{A}}\ddot{\theta}\,\hat{\mathbf{z}} = \overrightarrow{PG} \times (-\mathbf{a}_{\mathrm{P}} + m\mathbf{g}) + \mathbf{b} \times \mathbf{T} - \kappa\Delta\theta\,\hat{\mathbf{z}}, \tag{27}$$

where m, $\mathbf{g}$, $\mathbf{T}$, κ, and $\Delta\theta$ are mass, gravitational acceleration, the tension in the page, stiffness, and the amount of the angle displaced from the relaxed position. Neglecting the mass of paper, the tension equals the friction force between the page and the electroadhesive pad, which is given by

$$F_f = \begin{cases} \leq \mu_s N & \text{in stiction} \\ = \mu_k N & \text{in slip} \end{cases}, \tag{28}$$

where μ_s, μ_k, and N denote static friction coefficient, kinetic friction coefficient, and the normal force exerted by electroadhesive force, respectively. On the other hand, since a sheet of paper cannot withstand compression, the paper adhering to the electroadhesive pad can only slip out. Hence, the remaining length of the page is estimated as

$$y(t) = l_0 - \max_{t' \in [0,t]} \{x(t')\}, \tag{29}$$

where l_0 is the width of a page. Under the assumption that the electroadhesive force is uniformly distributed, the normal force is given as

$$N = N_0 y, \tag{30}$$

where N_0 is electroadhesive force per unit length.

From Eqs. (26) to (30), the motion of the electroadhesive pad is fully analyzed. The result shows that when the spring has low stiffness, the electroadhesive pad becomes unstable [Fig. 7(b)]. In stiction state, as long as a page does not bend, the machine is simplified into the four-bar linkage of double-rocker. As approaching to the dead point, the electroadhesive pad stores potential energy, and the tension in the page increases. When the increased tension overcomes the static friction, the transition from stick to slip occurs to initiate the rotational motion of the electroadhesive pad. The potential energy is being lost in the kinetic friction during the rotation, and it is continued until the page stops slipping out of the electroadhesive pad. Assuming the rotating arm rotates slowly, the angle at which the slip stops can be approximately obtained, using energy conservation, from

$$\int_{y_i}^{y_f} \mu_k N_0 y \, dy = \frac{1}{2} mgb\Delta(\sin\theta) + \frac{1}{2}\kappa\Delta\left((\theta - \theta_0)^2\right), \tag{31}$$

where y_i and y_f are the remaining length at the initial and final states, respectively. From Eq. (31), it is implied that the stick-slip instability can be minimized by reducing potential energy stored during the stiction or by increasing dissipation of the potential energy in kinetic friction. When the spring has high stiffness, the motion of the electroadhesive pad becomes stable, as the reduced amount of potential energy stores [Fig. 7(c)].

Even though the stick-slip instability is eliminated, if a page convexes upwards during the rotation, it is pulled and easily detached by the tension because of peeling effects [Fig. 8(a)]. The peeling effect significantly weakens the electroadhesive force in a similar way as zipping mechanism [11]. Especially, as the near-field electroadhesive force only penetrates tens of micrometers, once a part of a page is disengaged, the detached part is more unlikely to be reattached than in the case with the electroadhesive force that has large penetration depth. By tilting the electroadhesive pad largely enough, the page can convex downwards, and the tension keeps it from being peeled off [Fig. 8(b)]. Hence, the electroadhesive pad should be tilted at a large angle to have a positive deflection angle δ throughout the flattening process to avoid peeling, which is expressed as

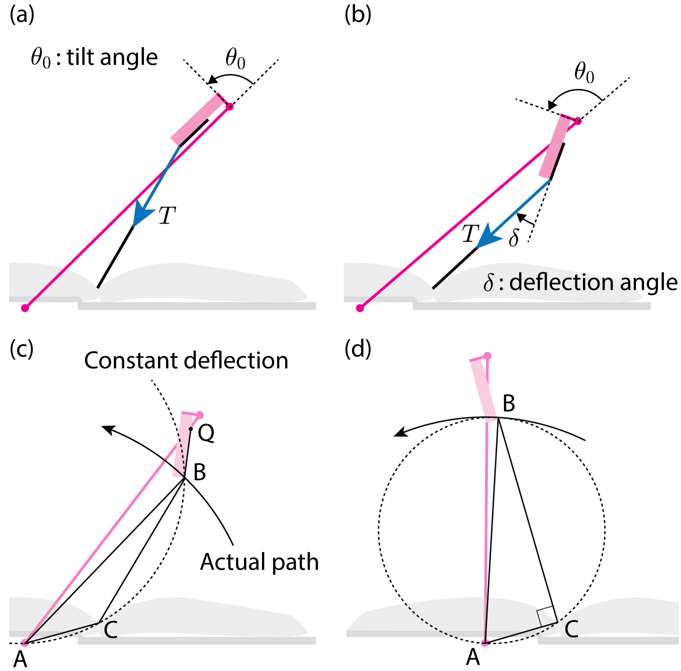

Fig. 8: (a) If the tilt angle is small, the tension in the page is applied in the direction of peeling the paper, which considerably drops the strength of the electroadhesive force. (b) When the tilt angle is sufficiently large, the tension prevents the paper from being peeled off to secure the electroadhesion. (c) As the actual path of the electroadhesive pad will be inside the circumscribed circle of triangle ABC, the deflection angle decreases. (d) When triangle ABC becomes a right triangle, the deflection angle is minimized since the circumcircle is tangent to the actual path.

$$\min \delta \geq 0. \tag{32}$$

Kinematic study shows that the deflection angle decreases [Fig. 8(c)]. The deflection angle is obtained by

$$\delta = (180^\circ - \angle ABQ) - \angle ABC, \tag{33}$$

where point B is the edge of the electroadhesive pad. When we neglect the small vibration caused by stick-slip, $\angle ABQ$ is fixed, and thus, finding the minimum deflection angle is equivalent to finding the maximum $\angle ABC$. If point B follows the circumscribed circle of $\triangle ABC$, $\angle ABC$ will not change. However actually, since the actual trajectory of point B is the circle centered at point A with radius $\overline{AB}$, point B will be inside the circumcircle to have larger $\angle ABC$. Hence, the deflection angle decreases.

The deflection angle is minimum when $\angle B$ is a right angle [Fig. 8(d)]. When $\triangle ABC$ is a right triangle, the diameter of the circumcircle is $\overline{AB}$. As the actual path is also the circle centered at point A, and the two circles are tangent, point B will not be in the circumscribed circle, and the deflection angle

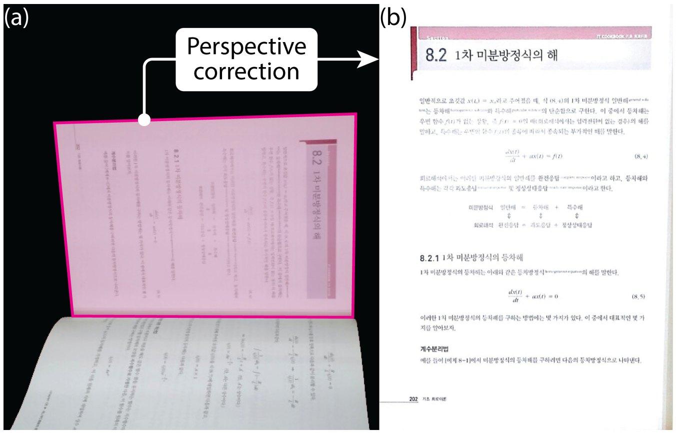

Fig. 9: (a) The image is acquired when the page is completely flat. The colored area is the region identified by the edge detection. (b) The result of image processing shows the page is flat enough for the acquired image to be successfully rectified by the perspective correction.

begins to increase. Hence, the deflection angle is minimized when $\angle B$ is a right angle. Therefore, Eq. (32) is simplified as

$$\delta \geq 0, \qquad \text{when } \angle C = 90^\circ. \tag{34}$$

From Eq. (34), the minimum tilt angle for preventing peeling can be determined.

V. Performance Evaluation

The result of the image processing shows that the page is flat enough to allow the perspective correction to be performed successfully [Fig. 9].

VI. Conclusion

In this paper, we study the ratio of electroadhesive forces on the closest paper to the second and show that in small length-scales, the force ratio is dominantly controlled by the period of electrode configurations regardless of the geometries. Based on the result, a double-sided structure is designed focusing on increasing the force ratio. Despite having the same spacing as interdigital patterns, the double-sided structure has half as small period as the interdigital patterns. The dynamic study on the electroadhesive pad shows that stick-slip instability arising from the friction can be minimized by employing a spring with high stiffness. In the kinematic study, the minimum tilt angle is determined to secure the electroadhesion from peeling effect. The experiment shows that our mechanism turns and flattens a page enough for successful perspective correction. We believe that our mechanism turning pages electronically can simplify conventional book scanners.

References

[1] B. Mandel, L. Belkhir, W. Burger, T. Sollitt, S. Miller, E. Kaminker, and T. Taylor, “Automatic book page turner for imaging,” Aug. 21 2013, eP Patent 1,438,835.

[2] S. Schramek, S. Quidenus, T. Aigner, and E. Pfarl, “Device for the digitalized recording of books,” Sep. 11 2015, wO Patent App. PCT/AT2014/050,056.

[3] K. Rieck, L. Belkhir, B. Hughner, and K. Rodas, “System and method for large format imaging,” Jul. 16 2009, uS Patent App. 12/353,753.

[4] L. Belkhir, “Page turning apparatus with a vacuum plenum and an adaptive air fluffer,” Sep. 29 2009, uS Patent 7,595,915.

[5] Y. Ishioka, “Booklet page turning apparatus, booklet page turning method, and booklet processing apparatus,” Jul. 24 2012, uS Patent 8,227,680.

[6] H. Wurm, T. Kramer, and W. Richter, “Mechanical device for turning pages,” Mar. 26 2014, eP Patent 2,493,697.

[7] Treventus, “Scan robot 2.0 mds.”

[8] Y. Watanabe, M. Tamei, M. Yamada, and M. Ishikawa, “Automatic page turner machine for high-speed book digitization,” in *2013 IEEE/RSJ International Conference on Intelligent Robots and Systems*. IEEE, 2013, pp. 272–279.

[9] H. Prahlad, R. Pelrine, S. Stanford, J. Marlow, and R. Kornbluh, “Electroadhesive robots?wall climbing robots enabled by a novel, robust, and electrically controllable adhesion technology,” in *Robotics and Automation, 2008. ICRA 2008. IEEE International Conference on*. IEEE, 2008, pp. 3028–3033.

[10] R. Chen, “A gecko-inspired electroadhesive wall-climbing robot,” *IEEE Potentials*, vol. 34, no. 2, pp. 15–19, 2015.

[11] K. H. Koh, M. Sreekumar, and S. Ponnambalam, “Hybrid electrostatic and elastomer adhesion mechanism for wall climbing robot,” *Mechatronics*, vol. 35, pp. 122–135, 2016.

[12] M. Graule, P. Chirarattananon, S. Fuller, N. Jafferis, K. Ma, M. Spenko, R. Kornbluh, and R. Wood, “Perching and takeoff of a robotic insect on overhangs using switchable electrostatic adhesion,” *Science*, vol. 352, no. 6288, pp. 978–982, 2016.

[13] J. Shintake, S. Rosset, B. Schubert, D. Floreano, and H. Shea, “Versatile soft grippers with intrinsic electroadhesion based on multifunctional polymer actuators,” *Advanced Materials*, vol. 28, no. 2, pp. 231–238, 2016.

[14] G. Monkman, P. Taylor, and G. Farnworth, “Principles of electroadhesion in clothing robotics,” *International Journal of Clothing Science and Technology*, vol. 1, no. 3, pp. 14–20, 1989.

[15] G. J. Monkman, “Robot grippers for use with fibrous materials,” *The International journal of robotics research*, vol. 14, no. 2, pp. 144–151, 1995.

[16] H. Prahlad, J. Eckerle, R. Kornbluh, and R. Pelrine, “Handling and sorting materials using electroadhesion,” Nov. 7 2013, uS Patent App. 13/886,058.

[17] K. Asano, F. Hatakeyama, and K. Yatsuzuka, “Fundamental study of an electrostatic chuck for silicon wafer handling,” *IEEE Transactions on Industry Applications*, vol. 38, no. 3, pp. 840–845, 2002.

[18] K. H. Koh, M. Sreekumar, and S. Ponnambalam, “Experimental investigation of the effect of the driving voltage of an electroadhesion actuator,” *Materials*, vol. 7, no. 7, pp. 4963–4981, 2014.

[19] A. Yamashita, A. Kawarago, T. Kaneko, and K. T. Miura, “Shape reconstruction and image restoration for non-flat surfaces of documents with a stereo vision system,” in *Pattern Recognition, 2004. ICPR 2004. Proceedings of the 17th International Conference on*, vol. 1. IEEE, 2004, pp. 482–485.

[20] F. Lefevere and M. Saric, “Detection of grooves in scanned images,” Mar. 24 2009, uS Patent 7,508,978.

[21] H. Shibayama, Y. Watanabe, and M. Ishikawa, “Reconstruction of 3d surface and restoration of flat document image from monocular image sequence,” in *Asian Conference on Computer Vision*. Springer, 2012, pp. 350–364.

[22] D. Qumsiyeh, “Linear book scanner,” Apr. 29 2014, uS Patent 8,711,448.

[23] H. Morgan, A. G. Izquierdo, D. Bakewell, N. G. Green, and A. Ramos, “The dielectrophoretic and travelling wave forces generated by interdigitated electrode arrays: analytical solution using fourier series,” *Journal of Physics D: Applied Physics*, vol. 34, no. 10, p. 1553, 2001.

[24] X. Wang, X.-B. Wang, F. Becker, and P. R. Gascoyne, “A theoretical method of electrical field analysis for dielectrophoretic

electrode arrays using green's theorem," *Journal of physics D: applied physics*, vol. 29, no. 6, p. 1649, 1996.

[25] J. P. D. Téllez, J. Krahn, and C. Menon, "Characterization of electro-adhesives for robotic applications," in *Robotics and Biomimetics (ROBIO), 2011 IEEE International Conference on*. IEEE, 2011, pp. 1867–1872.

[26] W. J. Tong, C. S. Chin, and W. P. Lin, "Design of a miniature tri-axis vertical wall structure climbing robot using electroadhesion," in *2014 9th IEEE Conference on Industrial Electronics and Applications*. IEEE, 2014, pp. 473–477.